Theoretical Study of Electron, Proton, and Proton-Coupled Electron Transfer in Iron Bi-imidazoline Complexes

Nedialka Iordanova, Hélène Decornez, and Sharon Hammes-Schiffer*

Contribution from the Department of Chemistry, 152 Davey Laboratory, The Pennsylvania State University, University Park, Pennsylvania 16802

Received January 4, 2001

Abstract: A comparative theoretical investigation of single electron transfer (ET), single proton transfer (PT), and proton-coupled electron transfer (PCET) reactions in iron bi-imidazoline complexes is presented. These calculations are motivated by experimental studies showing that the rates of ET and PCET are similar and are both slower than the rate of PT for these systems (Roth, J. P.; Lovel, S.; Mayer, J. M. *J. Am. Chem. Soc.* **2000**, *122*, 5486). The theoretical calculations are based on a multistate continuum theory, in which the solute is described by a multistate valence bond model, the transferring hydrogen nucleus is treated quantum mechanically, and the solvent is represented as a dielectric continuum. For electronically nonadiabatic electron transfer, the rate expressions for ET and PCET depend on the inner-sphere (solute) and outer-sphere (solvent) reorganization energies and on the electronic coupling, which is averaged over the reactant and product proton vibrational wave functions for PCET. The small overlap of the proton vibrational wave functions localized on opposite sides of the proton transfer interface decreases the coupling for PCET relative to ET. The theory accurately reproduces the experimentally measured rates and deuterium kinetic isotope effects for ET and PCET. The calculations indicate that the similarity of the rates for ET and PCET is due mainly to the compensation of the smaller outer-sphere solvent reorganization energy for PCET by the larger coupling for ET. The moderate kinetic isotope effect for PCET arises from the relatively short proton transfer distance. The PT reaction is found to be dominated by solute reorganization (with very small solvent reorganization energy) and to be electronically adiabatic, leading to a fundamentally different mechanism that accounts for the faster rate.

Introduction

Processes requiring the transfer of both a proton and an electron are ubiquitous throughout chemistry and biology.[1−20] Although these reactions entail the net transfer of a hydrogen atom, often the electron and proton transfer between different centers, resulting in significant charge rearrangement. In this paper, all reactions involving the transfer of both a proton and an electron are denoted proton-coupled electron transfer (PCET) in order to maintain generality. PCET reactions exhibit complex interactions among the transferring proton and electron, the solute electrons involved in the breaking and forming of chemical bonds, the solute vibrational modes, and the solvent. As a result, the investigation of PCET reactions is challenging from both a theoretical perspective and an experimental perspective. A critical step toward elucidating the fundamental principles of PCET is determining the relationship between PCET and the corresponding single charge transfer reactions.

Recently, Mayer and co-workers investigated this relationship by performing experiments on high-spin iron complexes of 2,2′-bi-imidazoline in acetonitrile.[14] They studied single electron transfer (ET), single proton transfer (PT), and PCET between the complexes shown in Chart 1. The specific reactions studied are

$$[Fe^{II}(H_2bim)]^{2+} + [Fe^{III}(H_2bim)]^{3+} \rightleftharpoons [Fe^{III}(H_2bim)]^{3+} + [Fe^{II}(H_2bim)]^{2+} \quad (1)$$

$$[Fe^{III}(H_2bim)]^{3+} + [Fe^{III}(Hbim)]^{2+} \rightleftharpoons [Fe^{III}(Hbim)]^{2+} + [Fe^{III}(H_2bim)]^{3+} \quad (2)$$

$$[Fe^{II}(H_2bim)]^{2+} + [Fe^{III}(Hbim)]^{2+} \rightleftharpoons [Fe^{III}(Hbim)]^{2+} + [Fe^{II}(H_2bim)]^{2+} \quad (3)$$

for single ET, single PT, and PCET, respectively. They used

* To whom correspondence should be addressed. E-mail: shs@chem.psu.edu.

(1) Babcock, G. T.; Barry, B. A.; Debus, R. J.; Hoganson, C. W.; Atamian, M.; McIntosh, L.; Sithole, I.; Yocum, C. F. *Biochemistry* **1989**, *28*, 9557.
(2) Okamura, M. Y.; Feher, G. *Annu. Rev. Biochem.* **1992**, *61*, 861.
(3) Kirmaier, C.; Holten, D. *The Photosynthetic Bacterial Reaction Center — Structure and Dynamics*; Plenum: New York, 1988.
(4) Wikstrom, M. *Nature* **1989**, *338*, 776.
(5) Babcock, G. T.; Wikstrom, M. *Nature* **1992**, *356*, 301.
(6) Malmstrom, B. G. *Acc. Chem. Res.* **1993**, *26*, 332.
(7) Therien, M. J.; Selman, M.; Gray, H. B.; Chang, I.-J.; Winkler, J. R. *J. Am. Chem. Soc.* **1990**, *112*, 2420.
(8) Ulstrup, J. *Charge Transfer Processes in Condensed Media*; Springer-Verlag: Berlin, 1979.
(9) Kirby, J. P.; Roberts, J. A.; Nocera, D. G. *J. Am. Chem. Soc.* **1997**, *119*, 9230.
(10) Cukier, R. I.; Nocera, D. G. *Annu. Rev. Phys. Chem.* **1998**, *49*, 337.
(11) Farrer, B. T.; Thorp, H. H. *Inorg. Chem.* **1999**, *38*, 2497.
(12) Binstead, R. A.; Moyer, B. A.; Samuels, G. J.; Meyer, T. J. *J. Am. Chem. Soc.* **1981**, *103*, 2897.
(13) Binstead, R. A.; Stultz, L. K.; Meyer, T. J. *Inorg. Chem.* **1995**, *34*, 546.
(14) Roth, J. P.; Lovel, S.; Mayer, J. M. *J. Am. Chem. Soc.* **2000**, *122*, 5486.
(15) Onuchic, J. N.; Beratan, D. N. *J. Chem. Phys.* **1990**, *92*, 722.
(16) Siegbahn, P. E. M.; Eriksson, L.; Himo, F.; Pavlov, M. *J. Phys. Chem. B* **1998**, *102*, 10622.
(17) Sjoberg, B. M.; Ekberg, M.; Persson, A.; Sahlin, M. *J. Inorg. Biochem.* **1999**, *74*, 51.
(18) Hirst, J.; Duff, J. L. C.; Jameson, G. N. L.; Kemper, M. A.; Burgess, B. K.; Armstrong, F. A. *J. Am. Chem. Soc.* **1998**, *120*, 7085.
(19) Cukier, R. I. *J. Phys. Chem.* **1995**, *99*, 16101.
(20) Beratan, D. N.; Onuchic, J.; Winkler, J. P.; Gray, H. B. *Science* **1992**, *258*, 1740.

10.1021/ja0100524 CCC: $20.00
Published on Web 03/29/2001

Chart 1

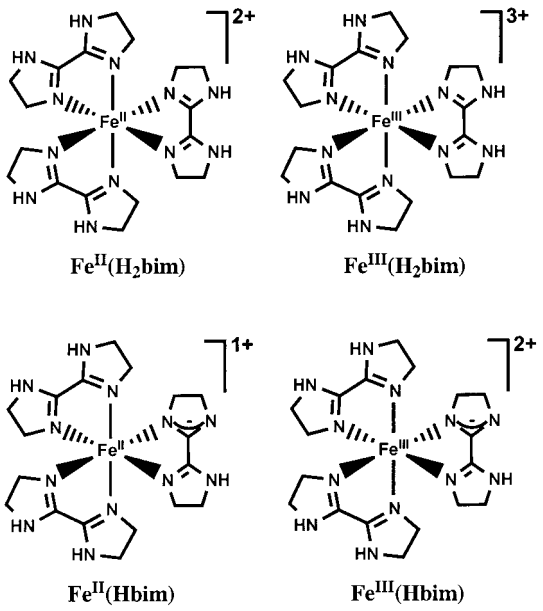

the dynamic NMR line-broadening technique to measure the rates for these three reactions. The rates measured at 298 K were 1.7 ($\pm$0.2) $\times$ 10^4, $\approx$ 2 $\times$ 10^6, and 5.8 ($\pm$0.6) $\times$ 10^3 M^{-1} s^{-1} for eqs 1, 2, and 3, respectively. These experiments provide a unique opportunity to make a comparative study of all three types of reactions.

One of the interesting results from these experiments is the finding that the rates for ET and PCET are similar in magnitude, compared to the much faster rate for PT. Mayer and co-workers explained this result in the context of adiabatic Marcus theory,[21,22] in which both ET and PCET are assumed to be electronically adiabatic (i.e., to occur on the electronic ground state). The contributions to the reaction barriers from both the solvent (outer-sphere) reorganization and the solute (inner-sphere) reorganization were investigated. The outer-sphere reorganization energy for the ET reaction was calculated from a simple two-sphere model,[22] leading to a value of 18 kcal/mol. The PCET reaction was viewed as a hydrogen atom transfer involving negligible solute charge rearrangement, so the outer-sphere reorganization energy for PCET was assumed to be zero. These outer-sphere reorganization energies, together with the experimentally determined free energy barriers, were used to calculate the inner-sphere reorganization energies from the standard adiabatic Marcus theory expression.[22−25] The calculated inner-sphere reorganization energies were 20 and 44 kcal/mol for the ET and PCET reactions, respectively. The larger inner-sphere reorganization energy for PCET was attributed to the N−H bond cleavage. Mayer and co-workers concluded that the similarity of the ET and PCET rates is due to the compensation of the larger outer-sphere reorganization energy for ET by the larger inner-sphere reorganization energy for PCET. In this paper, we present an alternative explanation for these experimental results.

Our approach is based on the recently developed multistate continuum theory for charge transfer processes.[26−29] In this theory, the solute is described by a multistate valence bond model, the transferring hydrogen nucleus is treated quantum mechanically, and the solvent is represented as a dielectric continuum. The outer-sphere reorganization energies are calculated with the frequency-resolved cavity model (FRCM),[30,31] which has been shown to provide accurate reorganization energies for electron transfer reactions. The rates for ET and PCET are calculated using rate expressions derived for the electronically nonadiabatic limit due to the relatively large distance ($\sim$10.3 Å) between the two iron centers. In this limit, the rate is proportional to the square of the coupling between the reactant and product states and is inversely proportional to the free energy barrier, which depends on the inner-sphere and outer-sphere reorganization energies. For the PCET reaction, the coupling is averaged over the reactant and product proton vibrational wave functions.[27]

The application of this theoretical approach to the iron biimidazoline complexes provides insight into the relation between the ET, PT, and PCET reactions. The outer-sphere reorganization energy for PCET calculated with the FRCM method is more than half of that for ET. This result indicates a significant change in solute charge distribution during PCET, suggesting that this is not a true "hydrogen atom" transfer. Thus, the PCET reaction may be viewed as the simultaneous transfer of an electron between the two iron centers and a proton between the two nitrogen atoms of the intervening proton transfer interface. The relatively small overlap of the reactant and product proton vibrational wave functions localized on opposite sides of the proton transfer interface decreases the coupling for PCET relative to ET. Our calculations imply that the similarity of the ET and PCET rates is due mainly to the compensation of the smaller outer-sphere reorganization energy for PCET by the larger coupling for ET. In addition to this comparison of the single ET and PCET reactions, we also investigate the single PT reaction. In contrast to the PCET reaction, the PT reaction is found to be dominated by solute reorganization and to be electronically adiabatic. These fundamental mechanistic differences account for the faster rate of single PT compared to PCET.

Theory and Methods

The theoretical framework used to describe ET, PT, and PCET reactions in this paper is based primarily on the recently developed multistate continuum theory.[26,28] As mentioned above, in this formulation the solute is described by a multistate valence bond model, the transferring hydrogen nucleus is treated quantum mechanically, and the solvent is represented as a dielectric continuum. This theory may be used to calculate the free energy surfaces for single ET or single PT as functions of a single collective solvent coordinate or to calculate the free energy surfaces for PCET as functions of two collective solvent coordinates corresponding to PT and ET, respectively. For the systems studied in this paper, the ET reaction is electronically nonadiabatic, and the PT reaction is electronically adiabatic. Rate expressions have been derived for single ET,[22−25,32] single PT,[33−35] and PCET[27,36]

(21) Marcus, R. A. *Annu. Rev. Phys. Chem.* **1964**, *15*, 155.
(22) Marcus, R. A.; Sutin, N. *Biochim. Biophys. Acta* **1985**, *811*, 265.
(23) Bixon, M.; Jortner, J. *Adv. Chem. Phys.* **1999**, *106*, 35.
(24) Barbara, P. F.; Meyer, T. J.; Ratner, M. A. *J. Phys. Chem.* **1996**, *100*, 13148.
(25) Newton, M. D.; Sutin, N. *Annu. Rev. Phys. Chem.* **1984**, *35*, 437.
(26) Soudackov, A. V.; Hammes-Schiffer, S. *J. Chem. Phys.* **1999**, *111*, 4672.
(27) Soudackov, A. V.; Hammes-Schiffer, S. *J. Chem. Phys.* **2000**, *113*, 2385.
(28) Hammes-Schiffer, S. In *Electron transfer in chemistry vol. I. principles, theories, methods, and techniques*; Balzani, V., Ed.; Wiley-VCH: Weinheim, 2001.
(29) Hammes-Schiffer, S. *Acc. Chem. Res.* **2001**, *34*, in press.
(30) Basilevsky, M. V.; Rostov, I. V.; Newton, M. D. *Chem. Phys.* **1998**, *232*, 189−199.
(31) Newton, M. D.; Basilevsky, M. V.; Rostov, I. V. *Chem. Phys.* **1998**, *232*, 201−210.
(32) Basilevsky, M. V.; Chudinov, G. E.; Newton, M. D. *Chem. Phys.* **1994**, *179*, 263−278.
(33) Warshel, A. *Computer Modeling of Chemical Reactions in Enzymes and Solutions*; John Wiley: New York, 1991.
(34) Borgis, D.; Hynes, J. T. *Chem. Phys.* **1993**, *170*, 315.

reactions in these regimes. Inner-sphere solute modes that are approximately harmonic and uncoupled to the solvent have been incorporated into the expressions for single ET[23] and PCET.[27] Within the framework of the multistate continuum theory,[27] the calculation of the rates requires the gas-phase valence bond matrix elements, the outer-sphere reorganization energies, the inner-sphere reorganization energies, and the work required to form the reacting complex in solution.

For the PCET reaction, the solute is represented by four diabatic states that are defined within a valence bond approach. The gas-phase valence bond matrix elements are based on a five-site model for the two hydrogen-bonded iron complexes:

$$Fe_D-N_D-H-N_A-Fe_A$$

where the D and A subscripts denote donor and acceptor, respectively. The four diabatic states are labeled 1*a*, 1*b*, 2*a*, and 2*b*, where the label 1 or 2 indicates that the electron is localized on Fe_D or Fe_A, respectively, and the label *a* or *b* indicates that the proton is bonded to N_D or N_A, respectively. The gas-phase valence bond matrix elements are represented by molecular mechanical terms fit to electronic structure calculations and experimental data. We emphasize that this five-site model is used only to provide molecular mechanical functional forms for the gas-phase matrix elements. As will be described below, all 122 atoms (or 121 atoms for the deprotonated form) of the iron bi-imidazoline complexes are included for the calculation of solvation properties.

The diagonal matrix elements are expressed as

$$\begin{aligned}(h_o)_{1a,1a} &= U^{\text{Morse}}_{N_DH} + U^{\text{rep}}_{N_AH} + U^{\text{Coul}}_{1a}\\ (h_o)_{1b,1b} &= U^{\text{Morse}}_{N_AH} + U^{\text{rep}}_{N_DH} + U^{\text{Coul}}_{1b} + \Delta E\\ (h_o)_{2a,2a} &= U^{\text{Morse}}_{N_DH} + U^{\text{rep}}_{N_AH} + U^{\text{Coul}}_{2a} + \Delta E\\ (h_o)_{2b,2b} &= U^{\text{Morse}}_{N_AH} + U^{\text{rep}}_{N_DH} + U^{\text{Coul}}_{2b}\end{aligned} \tag{4}$$

(Note that the dependence of the matrix elements on the proton coordinate r_p is suppressed in eq 4 for clarity.) The Morse potential for an N−H bond of length R_{NH} is

$$U^{\text{Morse}}_{NH}(r_p) = D_{NH}(1 - e^{-\beta_{NH}(R_{NH}-R^{\circ}_{NH})})^2 \tag{5}$$

where $D_{NH} = 93.0$ kcal/mol, $\beta_{NH} = 2.35$ Å^{-1}, and $R^{\circ}_{NH} = 1.00$ Å. These values were chosen to be consistent with the experimental dissociation energy, frequency, and equilibrium bond length for typical N−H bonds. The repulsion term between nonbonded atoms N and H separated by distance R_{NH} is

$$U^{\text{rep}}_{NH}(r_p) = D'_{NH}\, e^{-\beta'_{NH}R_{NH}} \tag{6}$$

where $\beta'_{NH} = 2.5$ Å^{-1} and $D'_{NH} = 300$ kcal/mol. The parameters for both the Morse and repulsion terms are similar to those used by Warshel and co-workers for related types of bonds.[33]

The Coulomb interaction potential between the transferring H atom and the other sites is

$$U^{\text{Coul}}_i(r_p) = \sum_k \frac{q^i_k q_H e^2}{R_{kH}} \tag{7}$$

where $\sum_k$ is a sum over all sites except the transferring hydrogen and the nitrogen bonded to the hydrogen, R_{kH} is the distance between the H atom and site *k*, q_H is the charge assigned to the hydrogen, q^i_k is the charge on site *k* for diabatic state *i*, and *e* represents the elementary charge. For all diabatic states, the charge on the H atom is +0.3, as obtained from a CHELPG charge analysis[37] on the isolated (H_2bim) ligand. The charge on each iron site is +2 or +3, depending on the oxidation state, and the charges on the N sites are −0.3 and −1.0 for the bonding and nonbonding atoms, respectively.

The constant ΔE is calculated from the equation $\Delta G^{\circ}_{1a\rightarrow 1b} = \Delta G^{\circ}_{1a\rightarrow 2a} = 11.5$ kcal/mol, where this number was determined electrochemically in ref 14. The quantity $\Delta G^{\circ}_{1a\rightarrow j}$ is the free energy difference between the solvated diabatic states *j* and 1*a* at the equilibrium solvent coordinates. By symmetry, $\Delta G^{\circ}_{1a\rightarrow 2b} = 0$ (indicating a thermoneutral reaction). These diabatic free energy differences are easily calculated within the multistate continuum theory.[26,28]

In this paper, the couplings between the diabatic states are assumed to be constant:

$$\begin{aligned}(h_o)_{1a,1b} &= (h_o)_{2a,2b} = V^{\text{PT}}\\ (h_o)_{1a,2a} &= (h_o)_{1b,2b} = V^{\text{ET}}\\ (h_o)_{1a,2b} &= (h_o)_{1b,2a} = V^{\text{EPT}}\end{aligned} \tag{8}$$

The value of the coupling V^{PT} was chosen to be similar in magnitude to the couplings used in other related EVB models and was refined to fit the experimental rate for the PCET reaction. The coupling V^{ET} was estimated by fitting to the experimental rate for the single ET reaction. For simplicity, in this paper the coupling for ET is assumed to be the same for the ET and PCET systems defined in eqs 1 and 3, which differ by only a proton. This assumption is reasonable if the distance between the iron centers is similar for the two systems. (In principle, the coupling V^{ET} could be calculated for each system using the generalized Mulliken−Hush formulation.[38,39]) Within the framework of valence bond theory,[33] V^{ETP} is expected to be significantly smaller than V^{ET} since V^{EPT} is a second-order coupling and V^{ET} is a first-order coupling. For simplicity, in this paper V^{EPT} was approximated as zero.

As mentioned above, all 122 atoms (or 121 atoms for the deprotonated form) of the iron bi-imidazoline complexes are included for the calculation of the solvation properties. The outer-sphere reorganization energies are calculated with the frequency-resolved cavity model (FRCM) developed by Newton, Rostov, and Basilevsky.[30,31] This approach allows us to consider distinct effective solute cavities pertaining to the optical and inertial solvent response. The cavities are formed from spheres centered on all of the atoms. The two effective radii for the solute atoms are defined as $r_\infty = \kappa r_{vdW}$ and $r_{in} = r_\infty + \delta$, where r_{vdW} is the van der Waals radius, κ is a universal scaling factor, and δ is a constant specific to the particular solvent. As given in ref 31, $\kappa = 0.9$ and $\delta = 1.8$ for acetonitrile. The static and optical dielectric constants of acetonitrile at 298 K are $\epsilon_o = 37.5$ and $\epsilon_\infty = 1.7999$. Assuming linear temperature dependence of these dielectric constants,[40,41] $\epsilon_o = 33.3$ and $\epsilon_\infty = 1.7565$ at 324 K. The charge density of each diabatic (i.e., valence bond) state is defined by assigning appropriate partial charges to all atoms. The reorganization energy matrix element between diabatic states *i* and *j* is determined by calculating the interaction of the charge density of state *i* with the dielectric continuum solvent response to the charge density of state *j*.

The atomic coordinates utilized for the FRCM calculations in this paper were obtained from the experimentally obtained crystal structure of the $Fe^{III}(H_2bim)$ complex.[14] To allow the hydrogen atoms to relax, the coordinates of only the hydrogen atoms were optimized at the ROHF level with the basis set LANL2DZ. (All electronic structure calculations in this paper were performed with the Gaussian98 program.[42]) This geometry was used for both reacting iron complexes, regardless of the oxidation state of the iron or the protonation state of the ligand, to maintain the symmetry of the system. (The outer-sphere theory of PCET used in this paper requires the solute nuclei other than the transferring hydrogen to be fixed, although the effects of inner-sphere solute modes are easily included in the rate expression.) The two iron complexes

(35) Borgis, D.; Tarjus, G.; Azzouz, H. *J. Phys. Chem.* **1992**, *96*, 3188.
(36) Cukier, R. I. *J. Phys. Chem.* **1996**, *100*, 15428.
(37) Breneman, C. M.; Wiberg, K. B. *J. Comput. Chem.* **1990**, *11*, 361.
(38) Cave, R. J.; Newton, M. D. *Chem. Phys. Lett.* **1996**, *249*, 15.
(39) Cave, R. J.; Newton, M. D. *J. Chem. Phys.* **1997**, *106*, 9213.
(40) Marcus, Y. *Ion Solvation*; John Wiley: New York, 1985.
(41) Matyushov, D. V.; Schmid, R. *Chem. Phys. Lett.* **1994**, *220*, 359.

were combined by imposing planarity of the two intervening ligands and an Fe−Fe distance of 10.3 Å (as determined from the experimental crystal structure for hydrogen-bonded Fe^{III}(Hbim)). We found that altering the angular orientation between the two intervening ligands and shifting the internal coordinates within the ligands to represent different iron oxidation states does not significantly impact the outer-sphere reorganization energies.

The atomic charges for the diabatic states used for the FRCM calculations in this paper were designated as follows. The iron atom was assigned a charge of +3 or +2 corresponding to the appropriate oxidation state. Note that this assignment neglects charge transfer between the iron and the ligands. Although this charge transfer is substantial, this simplification to the charge distribution does not qualitatively alter the calculated outer-sphere reorganization energies.[43] The atomic charges on the ligands were determined by performing electronic structure calculations on the isolated bi-imidazoline ligand H_2bim and the deprotonated ligand Hbim. The geometries of the H_2bim and Hbim ligands were optimized at the RHF/6-31G** level invoking C_{2v} and C_s symmetry, respectively, and the atomic charges were calculated with the CHELPG method[37] for the optimized ligands. These charges were used in a consistent manner to obtain partial atomic charges for all diabatic states.

The inner-sphere reorganization energy for the ET reaction due to the Fe−N bonds is estimated from the force constants of iron hexaamine complexes. The inner-sphere reorganization energy may be approximated as[22]

$$\lambda_{in} = \sum_j \frac{f_j^r f_j^p}{f_j^r + f_j^p} (\Delta q)^2 \tag{9}$$

where $\sum_j$ is a sum over relevant solute modes (assumed to be harmonic), f_j^r and f_j^p are the equilibrium force constants of the jth mode in the reactant and product, respectively, and Δq is the difference in reactant and product equilibrium bond lengths for the jth mode. The experimentally determined force constants for $[Fe(NH_3)_6]^{2+}$ and $[Fe(NH_3)_6]^{3+}$ are 148 and 232 kcal mol^{-1} Å^{-2}, respectively.[44] Mayer reports that $\Delta q = 0.1$ Å for the ET reaction in the iron bi-imidazoline complexes. Thus, the total inner-sphere reorganization energy for the reaction given in eq 1 is estimated as 10.8 kcal/mol. (Note that there are two six-coordinated iron complexes involved in this reaction, so a total of 12 iron−ligand bonds contribute to the inner-sphere reorganization energy.) We emphasize that this estimate is based on the assumption that the force constants are similar for NH_3 and bi-imidazoline ligands. If this assumption is valid, the frequency of the Fe−N bonds in the bi-imidazoline complex may be calculated by using half the mass of a bi-imidazoline ligand to obtain a frequency of ~200 cm^{-1}. Although this frequency is only slightly less than the thermal energy k_BT, we apply the classical treatment of the inner-sphere reorganization energy for our calculations.[24] This allows us to express the total reorganization energy as a sum of inner-sphere and outer-sphere reorganization energies.

The work w_r required to bring the two reacting iron complexes together is estimated from the expression[14,25,45]

$$w_r = \frac{e^2 Z_1 Z_2 f}{\epsilon_o r} \tag{10}$$

where Z_1 and Z_2 are the charges on each iron complex, r is the distance between the iron centers, ϵ_o is the static dielectric constant of the solvent, and f is the Debye screening factor defined as

$$f^{-1} = 1 + r\sqrt{\frac{8\pi N_A e^2 \mu}{10^{27} \epsilon_o k_B T}} \tag{11}$$

Here k_B is Boltzmann's constant (where k_BT is in kilocalories per mole), N_A is Avogadro's number, r is in angstroms, μ is the ionic strength (where $\mu = 0.1$ M for these systems),[14] and e represents the elementary charge, where $e^2 = 332.1$ kcal Å mol^{-1} after the appropriate unit conversions. This estimate of w_r is based on the assumption of spherical complexes. In our calculations, only a single value of w_r is calculated for the distance obtained from the experimentally obtained crystal structure of Fe^{III}(Hbim). In a more sophisticated treatment, the rate would be calculated by averaging over all orientations and distances within the reacting complex.

The rate constant for a bimolecular (second-order) electron transfer reaction may be expressed as[25,45]

$$k_{bi} = K_A(r) k_{uni} \tag{12}$$

where $K_A(r)$ is the equilibrium constant for the formation of the precursor complex (with separation distance r) and k_{uni} is the unimolecular (first-order) rate constant for electron transfer within this complex. (Note that this expression is valid only if the dissociation of the precursor complex is much faster than the electron transfer reaction.) The equilibrium constant $K_A(r)$ has been expressed as

$$K_A(r) = P_r \exp(-w_r / k_B T) \tag{13}$$

where w_r is defined in eq 10 and the prefactor P_r (which defines the standard state) may be approximated as

$$P_r = 4\pi N_A r^2 \delta r \times 10^{-27} \tag{14}$$

Here P_r is in units of inverse moles per liter, and r and δr are in angstroms, where δr is the range of distances over which the rate is appreciable. In this paper, $\delta r = 0.8$ Å, which has been shown to provide reasonable results.[45] For the separation of $r = 10.3$ Å used for the calculations in this paper, $P_r = 0.64$ M^{-1}. Note that this simplified description of the formation of the precursor complex neglects the formation of hydrogen bonds for single PT and PCET.

Results

In this section, we analyze the single ET, single PT, and PCET reactions for the iron bi-imidazoline system. In each case, the diabatic states are defined, and the appropriate rate expression is given. Consistent parameters are used to model all three types of reactions. The important differences among these types of reactions are illustrated through the free energy surfaces and proton potential energy profiles.

(42) Frisch, M. J.; Trucks, G. W.; Schlegel, H. B.; Scuseria, G. E.; Robb, M. A.; Cheeseman, J. R.; Zakrzewski, V. G.; Montgomery, J. A., Jr.; Stratmann, R. E.; Burant, J. C.; Dapprich, S.; Millam, J. M.; Daniels, A. D.; Kudin, K. N.; Strain, M. C.; Farkas, O.; Tomasi, J.; Barone, V.; Cossi, M.; Cammi, R.; Mennucci, B.; Pomelli, C.; Adamo, C.; Clifford, S.; Ochterski, J.; Petersson, G. A.; Ayala, P. Y.; Cui, Q.; Morokuma, K.; Malick, D. K.; Rabuck, A. D.; Raghavachari, K.; Foresman, J. B.; Cioslowski, J.; Ortiz, J. V.; Stefanov, B. B.; Liu, G.; Liashenko, A.; Piskorz, P.; Komaromi, I.; Gomperts, R.; Martin, R. L.; Fox, D. J.; Keith, T.; Al-Laham, M. A.; Peng, C. Y.; Nanayakkara, A.; Gonzalez, C.; Challacombe, M.; Gill, P. M. W.; Johnson, B.; Chen, W.; Wong, M. W.; Andres, J. L.; Gonzalez, C.; Head-Gordon, M.; Replogle, E. S.; Pople, J. A.*Gaussian 98*, Revision A.6; Gaussian, Inc.: Pittsburgh, PA, 1998.

(43) To test the sensitivity of the calculated outer-sphere reorganization energy to the specific choice of atomic charges, we also calculated the outer-sphere reorganization energy for single ET using charges obtained with the CHELPG method for partially optimized iron bi-imidazoline complexes. Although the CHELPG charges on the iron atoms are less than +1 for both oxidation states, we found that the outer-sphere reorganization energy is only ~2.5 kcal/mol smaller than the outer-sphere reorganization energy calculated with our model, in which the charges on the iron atoms are +2 and +3. Thus, the detailed charge distribution within each iron bi-imidazoline complex does not qualitatively impact the calculated outer-sphere reorganization energy.

(44) Zhou, Z.; Khan, S. U. M. *J. Phys. Chem.* **1989**, *93*, 5292.

(45) Sutin, N. *Prog. Inorg. Chem.* **1983**, *30*, 441.

Single ET Reaction. The single ET reaction in eq 1 may be described in terms of two diabatic states,

$$\begin{aligned} &(1) \qquad [Fe^{II}(H_2bim)]^{2+} + [Fe^{III}(H_2bim)]^{3+} \\ &(2) \qquad [Fe^{III}(H_2bim)]^{3+} + [Fe^{II}(H_2bim)]^{2+} \end{aligned} \tag{15}$$

The distance between the iron centers is assumed to be 10.3 Å, the distance in the experimentally obtained crystal structure for Fe^{III}(Hbim).[14] Steric interaction between the hydrogen atoms on the ligands would most likely prevent a smaller distance.

At this distance, the ET reaction is expected to be electronically nonadiabatic (i.e., the coupling between the diabatic states is much less than the thermal energy k_BT). For comparison, Newton[46] calculated an electronic coupling of ~25 cm^{-1} (0.07 kcal/mol), which is in the electronically nonadiabatic regime at 298 K, for iron hexa-aquo complexes at distances of ~7.0 Å. In addition, preliminary generalized Mulliken−Hush calculations on the iron bi-imidazoline complexes studied in this paper suggest that the electronic couplings are in the electronically nonadiabatic regime at 298 K.[47] Another indication that this ET reaction is electronically nonadiabatic is that substitution of the calculated total reorganization energy given below into the rate expression for electronically adiabatic ET does not reproduce the experimentally determined rate.[14]

An electronically nonadiabatic ET reaction is described as a nonadiabatic transition from diabatic state 1 to diabatic state 2. The simplest unimolecular rate expression for nonadiabatic ET is[22−25]

$$k_{uni}^{ET} = \frac{2\pi}{\hbar}|V_{12}|^2(4\pi\lambda k_BT)^{-1/2}\exp\left\{\frac{-\Delta G^\dagger}{k_BT}\right\} \tag{16}$$

where V_{12} is the coupling between the diabatic states, λ is the total reorganization energy, and $\Delta G^\dagger$ is the barrier defined as

$$\Delta G^\dagger = \frac{(\Delta G^\circ + \lambda)^2}{4\lambda} \tag{17}$$

The value of w_r, the work to form the precursor complex, is 2.02 kcal/mol at 298 K when calculated using the approach described above.

In standard outer-sphere Marcus theory,[21,22] the diabatic free energy curves for ET are parabolic as functions of a collective solvent coordinate z_e, which represents the difference between the electrostatic interaction energies of the two diabatic states with the solvent polarization. Figure 1 depicts the free energy curves calculated for the ET reaction studied in this paper, where $\Delta G^\circ = 0$. The outer-sphere reorganization energy, $\lambda_o = 13.1$ kcal/mol, calculated with the FRCM method, is indicated in this figure. When the inner-sphere modes are assumed to be uncoupled to the solvent and harmonic with frequencies much less than the thermal energy k_BT (i.e., the classical limit), the total reorganization energy in eq 16 may be expressed as a sum of outer-sphere and inner-sphere components:

$$\lambda = \lambda_o + \lambda_i \tag{18}$$

The inner-sphere reorganization energy due to the Fe−N bonds

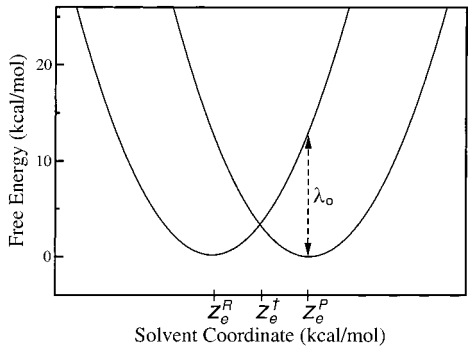

Figure 1. Diabatic free energy surfaces as functions of a collective solvent coordinate z_e for the single ET reaction in eq 1. The outer-sphere reorganization energy λ_o is indicated.

estimated with the method described above is $\lambda_i = 10.8$ kcal/mol, so the total reorganization energy is $\lambda = 23.9$ kcal/mol. The coupling for the ET reaction was determined from eq 16, with the values of w_r and λ given above used in conjunction with the experimentally determined rate. The resulting coupling is $V^{ET} = 0.025$ kcal/mol, which is similar in magnitude to electronic couplings calculated for iron hexa-aquo complexes.[46] Thus, the electronically nonadiabatic ET rate expression reproduces the experimentally determined rate with our calculated reorganization energies in conjunction with a physically reasonable value for the electronic coupling.

Single PT Reaction. The single PT reaction in eq 2 may be described in terms of two diabatic states,

$$\begin{aligned} &(a) \qquad [Fe^{III}(H_2bim)]^{3+} + [Fe^{III}(Hbim)]^{2+} \\ &(b) \qquad [Fe^{III}(Hbim)]^{2+} + [Fe^{III}(H_2bim)]^{3+} \end{aligned} \tag{19}$$

Typically proton transfer reactions are electronically adiabatic, and the electronically adiabatic states are mixtures of the *a* and *b* diabatic states. This type of PT reaction evolves along the ground electronic adiabatic state, where the reactant corresponds to an adiabatic state dominated by diabatic state *a* and the product corresponds to an adiabatic state dominated by diabatic state *b*. The transition state theory unimolecular rate expression for single PT is

$$k_{uni}^{PT} = \frac{k_BT}{h}\exp\left\{\frac{-\Delta G^\dagger}{k_BT}\right\} \tag{20}$$

where $\Delta G^\dagger$ is the barrier due to both solvent and solute reorganization. The calculated value of the work w_r for the formation of the precursor complex in solution for this PT reaction is 2.02 kcal/mol at 298 K (again assuming an Fe−Fe distance of 10.3 Å). The experimental rate for this single PT reaction indicates that $\Delta G^\dagger \approx 9$ kcal/mol for this reaction.

We have applied a theory for outer-sphere PT to this reaction.[28] The theory we utilized includes the nuclear quantum effects of the transferring hydrogen. In this formulation, the solvent polarization influences the proton potential energy curves, which determine the energies of the proton vibrational states. Analogous to the theory for single ET discussed above, the vibrationally adiabatic free energy curves are determined as functions of a collective solvent coordinate z_p, which represents the difference between the electrostatic interaction energies of the two diabatic states with the solvent polarization. The outer-sphere reorganization energy for PT calculated with the FRCM method is 2.4 kcal/mol. This solvent reorganization energy is substantially smaller than that for ET since the proton

(46) Newton, M. D. *J. Phys. Chem.* **1988**, *92*, 3049.

(47) Cave, R. J., private communication. The preliminary generalized Mullliken−Hush calculations are based on ZINDO wave functions, which exhibit considerable mixing between the iron d-orbitals and ligands for the highest energy occupied orbitals. Determination of whether this is an accurate picture for these systems will require more detailed studies of the geometry and method dependence of these results.

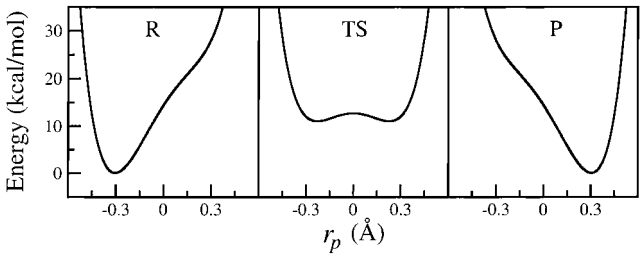

Figure 2. Proton potential energy curves as functions of the proton coordinate r_p for the reactant, transition state, and product geometries optimized at the B3LYP/6-31G** level for a pair of H_2bim−Hbim ligands in the gas phase.

is transferred only ∼0.3 Å, while the electron is transferred ∼10.3 Å. Thus, the charge distribution of the solute is altered more by the transfer of the electron than by the transfer of the proton. In addition, the solvent reorganization energy for this PT reaction is particularly small due to the presence of the bulky iron complexes, which prevent solvent from approaching close to the transferring proton. As a result of this small reorganization energy, we found that there is no barrier along the solvent coordinate z_p. This result implies that the barrier for this reaction is dominated by solute reorganization (i.e., changes in the bond lengths and angles within the ligands) rather than solvent reorganization.

To investigate the barrier due to solute reorganization for the single PT reaction, we performed electronic structure calculations for proton transfer between an isolated pair of planar (H_2bim)−(Hbim) ligands in the gas phase. To simulate PT within the precursor complex, the N−N distance was constrained to be 2.67 Å, the distance in the experimentally obtained crystal structure of Fe^{III}(Hbim). We optimized the transition state (in which the hydrogen atom is centered between the two ligands) and the reactant (in which the hydrogen atom is bonded to one of the nitrogen atoms) at the B3LYP/6-31G** level, maintaining C_s symmetry. We found that the difference between the optimized transition state and reactant structures is 8.8 kcal/mol (neglecting entropy and nuclear quantum effects). This barrier, together with the value of the work w_r (given above) for the formation of the precursor complex, is slightly higher than that indicated by the experimentally determined rate. We emphasize that the value of this barrier is not quantitatively accurate for the reaction in eq 2 due to the extremely simplified model that does not include the remainder of the iron complexes or the entropic, solvent, and nuclear quantum effects. A more sophisticated treatment of this reaction could be performed by using mixed quantum/classical methods that include nuclear quantum effects, the entire reacting complex, both solute and solvent reorganization, and dynamical effects. This type of treatment is beyond the scope of this paper.

The main purpose for this simplified gas-phase calculation is to illustrate the fundamental mechanism of the single PT reaction. Figure 2 provides the proton potential energy curves as functions of the proton coordinate r_p for the reactant, transition state, and product gas-phase structures. These proton potential energy curves were obtained by fixing the positions of all nuclei to the optimized structure and moving the transferring proton along a one-dimensional grid connecting the donor and acceptor N atoms. This figure indicates that the single PT reaction requires the symmetrization of the proton potential energy curve through solute reorganization. Note that the barrier along the proton coordinate is very low at the transition state, suggesting that the zero-point energy will be higher than the barrier. This result implies that the proton transfer reaction is

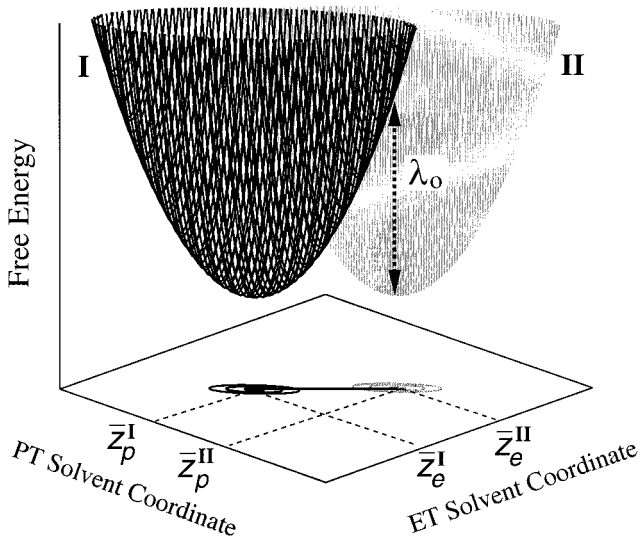

Figure 3. ET diabatic free energy surfaces as functions of two collective solvent coordinates, z_p and z_e, for the PCET reaction in eq 3. The lowest energy reactant (I) and product (II) free energy surfaces are shown. The minima for the reactant and product surfaces, respectively, are $(\bar{z}_p^I,\bar{z}_e^I)$ and $(\bar{z}_p^{II},\bar{z}_e^{II})$. The outer-sphere reorganization energy λ_o for these two surfaces is indicated.

vibrationally adiabatic (i.e., the system remains in the lowest proton vibrational state during the reaction).

PCET Reaction. The PCET reaction in eq 3 may be described in terms of four diabatic states,

$$\begin{aligned} &(1a) \quad [Fe^{II}(H_2bim)]^{2+} + [Fe^{III}(Hbim)]^{2+} \\ &(1b) \quad [Fe^{II}(Hbim)]^{+} + [Fe^{III}(H_2bim)]^{3+} \\ &(2a) \quad [Fe^{III}(H_2bim)]^{3+} + [Fe^{II}(Hbim)]^{+} \\ &(2b) \quad [Fe^{III}(Hbim)]^{2+} + [Fe^{II}(H_2bim)]^{2+} \end{aligned} \tag{21}$$

where 1 and 2 denote the ET state, and *a* and *b* denote the PT state. Thus, $1a \rightarrow 1b$ represents PT, $1a \rightarrow 2a$ represents ET, and $1a \rightarrow 2b$ represents EPT (where both the proton and the electron are transferred). Note that the ET and PT reactions represented by these diabatic states involve complexes chemically different than those described for the single ET and single PT reactions studied experimentally (as evidenced by comparison to the diabatic states in eqs 15 and 19).

As shown in ref 26, the free energy surfaces for PCET reactions may be calculated as functions of two collective solvent coordinates z_p and z_e, corresponding to PT and ET, respectively. For the systems studied in this paper, the PT reaction is electronically adiabatic, while the ET/EPT reactions are electronically nonadiabatic. In this case, the ET diabatic free energy surfaces corresponding to ET states 1 and 2 are calculated as mixtures of the *a* and *b* PT states. The reactants (I) are mixtures of the 1*a* and 1*b* diabatic states, and the products (II) are mixtures of the 2*a* and 2*b* states. The proton vibrational states are calculated for both the reactant (I) and product (II) ET diabatic surfaces, resulting in two sets of two-dimensional free energy surfaces that are approximate paraboloids. Figure 3 depicts the calculated lowest energy reactant and product free energy surfaces as functions of the two collective solvent coordinates.

In this theoretical formulation, the PCET reaction is described in terms of nonadiabatic transitions from the reactant (I) to the product (II) ET diabatic surfaces. (Here the ET diabatic states

I and II, respectively, may be viewed as the reactant and product PCET states.) In this paper, EPT refers to the transfer of an electron and a proton between pure diabatic states (i.e., $1a \rightarrow 2b$), while PCET refers to a transition between ET diabatic states (i.e., I → II or $1a/1b \rightarrow 2a/2b$). Note that hydrogen bonding in the precursor complex leads to substantial mixing between the *a* and *b* PT states in the reactant and product PCET states. For the iron bi-imidazoline systems studied in this paper, the lowest energy reactant PCET state is composed of 66% 1*a* and 34% 1*b* diabatic state. As will be discussed below, this substantial mixing influences the outer-sphere reorganization energies and the couplings for the PCET reaction.

The unimolecular rate expression derived in ref 27 for PCET is

$$k_{\text{uni}}^{\text{PCET}} = \frac{2\pi}{\hbar}\sum_{\mu} P_{\text{I}\mu}\sum_{\nu} V_{\mu\nu}^2(4\pi\lambda_{\mu\nu}k_{\text{B}}T)^{-1/2}\exp\left\{\frac{-\Delta G_{\mu\nu}^{\dagger}}{k_{\text{B}}T}\right\} \tag{22}$$

where $\sum_{\mu}$ and $\sum_{\nu}$ indicate a sum over vibrational states associated with ET states 1 and 2, respectively, $P_{\text{I}\mu}$ is the Boltzmann factor for state Iμ, and

$$\Delta G_{\mu\nu}^{\dagger} = \frac{(\Delta G_{\mu\nu}^{\circ} + \lambda_{\mu\nu})^2}{4\lambda_{\mu\nu}} \tag{23}$$

In this expression the free energy difference is defined as

$$\Delta G_{\mu\nu}^{\circ} = \epsilon_{\nu}^{\text{II}}(\bar{z}_{\text{p}}^{\text{II}\nu},\bar{z}_{\text{e}}^{\text{II}\nu}) - \epsilon_{\mu}^{\text{I}}(\bar{z}_{\text{p}}^{\text{I}\mu},\bar{z}_{\text{e}}^{\text{I}\mu}) \tag{24}$$

where $(\bar{z}_{\text{p}}^{\text{I}\mu},\bar{z}_{\text{e}}^{\text{I}\mu})$ and $(\bar{z}_{\text{p}}^{\text{II}\nu},\bar{z}_{\text{e}}^{\text{II}\nu})$ are the solvent coordinates for the minima of the ET diabatic free energy surfaces $\epsilon_{\mu}^{\text{I}}(z_{\text{p}},z_{\text{e}})$ and $\epsilon_{\nu}^{\text{II}}(z_{\text{p}},z_{\text{e}})$, respectively. Moreover, the total reorganization energy is expressed as the sum of the outer-sphere and inner-sphere contributions in the classical limit:

$$\lambda_{\mu\nu} = (\lambda_{\text{o}})_{\mu\nu} + \lambda_{\text{i}} \tag{25}$$

where the outer-sphere reorganization energy is defined as

$$(\lambda_{\text{o}})_{\mu\nu} = \epsilon_{\mu}^{\text{I}}(\bar{z}_{\text{p}}^{\text{II}\nu},\bar{z}_{\text{e}}^{\text{II}\nu}) - \epsilon_{\mu}^{\text{I}}(\bar{z}_{\text{p}}^{\text{I}\mu},\bar{z}_{\text{e}}^{\text{I}\mu}) = \epsilon_{\nu}^{\text{II}}(\bar{z}_{\text{p}}^{\text{I}\mu},\bar{z}_{\text{e}}^{\text{I}\mu}) - \epsilon_{\nu}^{\text{II}}(\bar{z}_{\text{p}}^{\text{II}\nu},\bar{z}_{\text{e}}^{\text{II}\nu}) \tag{26}$$

The outer-sphere reorganization energy for the lowest two ET diabatic free energy surfaces is indicated in Figure 3. For this pair of states, $\Delta G^{\circ} = 0$. The coupling $V_{\mu\nu}$ in the PCET rate expression given in eq 22 is defined as

$$V_{\mu\nu} = \langle\phi_{\mu}^{\text{I}}|V(r_{\text{p}},z_{\text{p}}^{\dagger})|\phi_{\nu}^{\text{II}}\rangle_{\text{p}} \tag{27}$$

where the subscript of the angular brackets indicates integration over r_{p}, $z_{\text{p}}^{\dagger}$ is the value of z_{p} in the intersection region, and ϕ_{μ}^{I} and ϕ_{ν}^{II} are the proton vibrational wave functions for the reactant and product ET diabatic states, respectively. For symmetric PCET systems,

$$V(r_{\text{p}},z_{\text{p}}^{\dagger}) = (c_{1a}c_{2a} + c_{1b}c_{2b})V^{\text{ET}} + (c_{1a}c_{2b} + c_{1b}c_{2a})V^{\text{EPT}} \tag{28}$$

where each coefficient c_i denotes the weighting of the diabatic state *i* in the reactant or product ET diabatic state and depends on the proton coordinate r_{p}. Note that the coupling term for the PCET reaction is averaged over the reactant and product proton vibrational wave functions. The overlap of the reactant and proton vibrational wave functions plays a role similar to that of the Franck−Condon overlap factor in theories including quantum mechanical inner-sphere modes for single ET.

Table 1. Calculated Outer-Sphere Reorganization Energies (kcal/mol) between the Indicated Diabatic States for the Single ET, Single PT, and PCET Reactions

ET[a]	PT[b]	PCET[c]		
$\lambda_{1\rightarrow 2}^{\text{ET}}$	$\lambda_{a\rightarrow b}^{\text{PT}}$	$\lambda_{1a\rightarrow 2a}^{\text{ET}}$	$\lambda_{1a\rightarrow 1b}^{\text{PT}}$	$\lambda_{1a\rightarrow 2b}^{\text{EPT}}$
13.1	2.4	13.0	2.4	5.8

[a] Diabatic states defined in eq 15. [b] Diabatic states defined in eq 19. [c] Diabatic states defined in eq 21.

In our calculations, V^{ET} is assumed to be the same for PCET as for ET, and V^{EPT} is approximated as zero. (As mentioned above, V^{EPT} is expected to be substantially smaller than V^{ET} since V^{EPT} is a second-order coupling and V^{ET} is a first-order coupling.) For the iron bi-imidazoline system studied in this paper, $V(r_{\text{p}},z_{\text{p}}^{\dagger}) = 0.99V^{\text{ET}}$ for the lowest energy reactant and product ET diabatic states at $r_{\text{p}} = 0$ (corresponding to maximum overlap of the proton vibrational wave functions). The prefactor is nearly unity due to substantial mixing of the *a* and *b* PT states in the ET diabatic states. Thus, the overall coupling between these two free energy surfaces may be approximated as $V_{\mu\nu} \approx V^{\text{ET}}\langle\phi_{\mu}^{\text{I}}|\phi_{\nu}^{\text{II}}\rangle_{\text{p}}$. This analysis illustrates that the smaller coupling for PCET compared to ET is due mainly to the averaging over the reactant and product proton vibrational wave functions for PCET.

The outer-sphere reorganization energies between the diabatic states representing the reaction from 1*a* to 1*b* (PT), 1*a* to 2*a* (ET), and 1*a* to 2*b* (EPT) are given in Table 1. Note that the outer-sphere reorganization energies for PT and ET in this system are very similar to those for the single PT and single ET reactions discussed above. This similarity indicates that the oxidation state of the iron does not significantly impact the reorganization energy of the PT reaction, and the protonation state of the ligand does not significantly impact the reorganization energy of the ET reaction. Also note that the outer-sphere reorganization energy for EPT is not zero, as assumed by Mayer and co-workers. This result implies that the solute charge redistribution during the PCET reaction is significant. Moreover, as will be shown below, the outer-sphere reorganization energy for the overall PCET reaction is between those for ET and EPT since the reactant and product ET diabatic states are mixtures of the *a* and *b* PT states.

The values for the parameters required to evaluate eq 22 are calculated in the same way as for the single ET and single PT reactions. The calculated value for w_{r} (assuming an Fe−Fe distance of 10.3 Å) at 298 K is 1.35 kcal/mol. This value differs from that calculated for the single ET and single PT reactions since the charges on the two reacting iron complexes are +3 and +2 for the single ET and single PT reactions, but are +2 and +2 for the PCET reaction. The inner-sphere reorganization energy due to the Fe−N bonds is estimated to be the same as that for the single ET reaction. The value of ΔE was set to 0.2 kcal/mol in order to reproduce the experimentally determined free energy difference between solvated diabatic states 1*a* and 1*b* (or, equivalently, 1*a* and 2*a*). The coupling V^{ET} is set to the value of the coupling V_{12} determined for the single ET reaction, and the coupling V^{EPT} is assumed to be much smaller than V^{ET} and thus is approximated as zero. Thus, the only flexible parameter for this PCET model is the coupling V^{PT}, which influences the mixing between the *a* and *b* PT states within the reactant and product ET diabatic states. Starting with a value similar to that used for related proton transfer reactions described

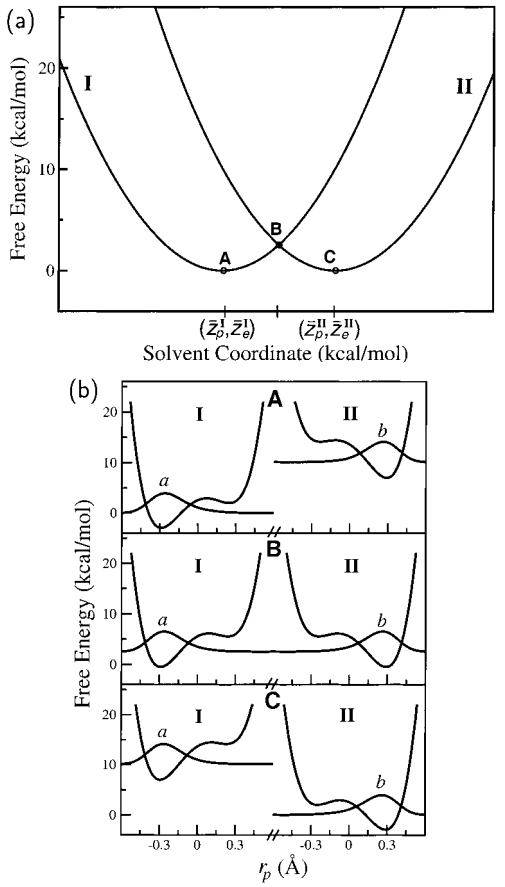

Figure 4. (a) Slice of the two-dimensional ET diabatic free energy surfaces shown in Figure 3 along the line connecting the two minima. The lowest energy reactant (I) and product (II) free energy surfaces are shown. Points A, B, and C represent the equilibrium reactant configuration, the intersection point, and the equilibrium product configuration, respectively. (b) Proton potential energy curves and corresponding ground state proton vibrational wave functions as functions of the proton coordinate r_p for the solvent coordinates associated with points A, B, and C indicated in (a). The proton potential energy curves are labeled I (or II) to denote the reactant (or product) ET diabatic free energy surface. The proton vibrational wave functions are labeled *a* or *b* to indicate the dominant PT state.

by empirical valence bond potentials,[33,48] we refined V^{PT} to reproduce the rate for the PCET reaction in eq 21 at 298 K. The resulting coupling is $V^{PT} = 60$ kcal/mol. (Note that varying V^{PT} within a reasonable range does not change the order of magnitude of the rate but rather is used simply for fine-tuning to reproduce the exact experimental rate.) Without further fitting, we calculated the deuterium kinetic isotope effect at 324 K and obtained a value of 2.36, which reproduces the experimentally determined value of 2.3 ± 0.3 remarkably well.

The mechanism of the PCET reaction may be determined by analyzing slices of the two-dimensional ET diabatic free energy surfaces. Figure 4a depicts a slice of the calculated two-dimensional free energy surfaces for the PCET reaction. This slice connects the minima of the two lowest ET diabatic surfaces shown in Figure 3, so the reaction coordinate is diagonal in the two-dimensional solvent space. For simplicity, the dependence of the free energy surfaces on the inner-sphere coordinates representing the Fe−N motion is not included in the figures. In the derivation of the rate expression for PCET,[27] these inner-sphere coordinates are assumed to be uncoupled to both the proton and solvent coordinates and thus do not influence the shapes of the free energy surfaces along the solvent coordinates or the proton vibrational wave functions.

(48) Schmitt, U.; Voth, G. A. *J. Chem. Phys.* **1999**, *111*, 9361.

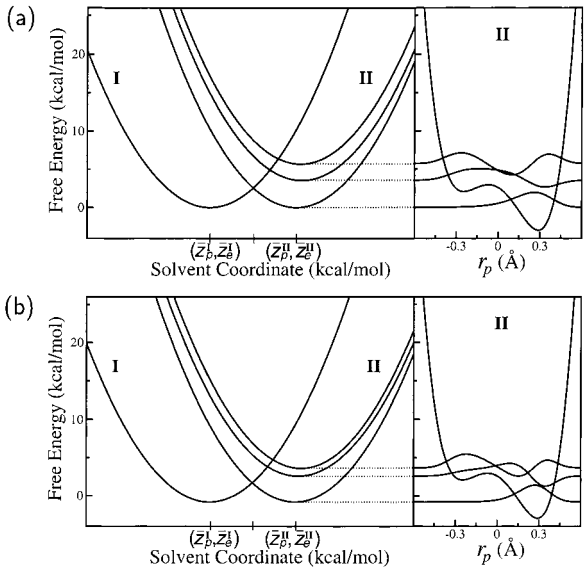

Figure 5. Slices of the two-dimensional ET diabatic free energy surfaces shown in Figure 3 along the line connecting the two minima for (a) hydrogen and (b) deuterium. On the left are the free energy surfaces as functions of the solvent coordinates, including the lowest energy reactant (I) free energy surface and the three lowest product (II) free energy surfaces. On the right are the product (II) proton potential energy curves and the corresponding proton vibrational wave functions as functions of the proton coordinate r_p evaluated at the minimum of the ground state product free energy surface. Note that the energies associated with the proton vibrational wave functions coincide with the energies of the product free energy surfaces.

Figure 4b shows the reactant and product proton potential energy curves (labeled I and II, respectively) and the corresponding proton vibrational wave functions as functions of the proton coordinate r_p for select solvent coordinates (z_p,z_e). The asymmetry of these proton potential energy curves is due to the different oxidation states (+2 and +3) of the iron atoms on each side of the proton transfer interface. As a result of electrostatic interactions, in ET state 1 (where the donor iron atom has oxidation state +2) the *a* well is lower in energy, while in ET state 2 (where the acceptor iron atom has oxidation state +2) the *b* well is lower in energy. Thus, in the reactant (I) proton potential energy curve the *a* well is lower in energy, while in the product (II) proton potential energy curve the *b* well is lower in energy. As a result, the lowest reactant proton vibrational wave function is localized in the *a* well, while the lowest product proton vibrational wave function is localized in the *b* well. This asymmetry remains along the entire PCET reaction path, regardless of the solvent coordinates. On the other hand, Figure 4b shows that altering the solvent coordinates along the reaction path influences the relative energies of the reactant and product vibrational states. At the intersection point of the free energy surfaces, the ground vibrational states for the reactant and product are degenerate. The nonadiabatic transition between these two surfaces represents simultaneous quantum mechanical tunneling of a proton and an electron.

Excited product vibrational states also play a role in the PCET reaction. Figure 5a depicts the lowest reactant and the three lowest product PCET free energy surfaces. Adjacent to these free energy profiles is the product proton potential energy curve with associated proton vibrational wave functions evaluated at the solvent coordinates corresponding to the minimum of the lowest product free energy surface. Note that the energies of

Table 2. Analysis of Contributions to PCET Rate for H and D at 298 and 324 K (Energies in kcal/mol)

isotope	product state	contribution to rate (%)	ΔG° [a]	λ_o [b]	V^2 [c]	$e^{-\Delta G^\ddagger/k_BT}$ [d]
H	1	53	0	10.1	9.6×10^{-6}	1.5×10^{-5}
(298 K)	2	44	3.5	11.5	3.4×10^{-4}	3.6×10^{-7}
	3	3	5.6	11.1	2.1×10^{-4}	4.6×10^{-8}
H	1	45	0	10.2	9.1×10^{-6}	2.8×10^{-5}
(324 K)	2	50	3.5	11.6	3.3×10^{-4}	8.5×10^{-7}
	3	5	5.7	11.3	2.2×10^{-4}	1.3×10^{-7}
D	1	4	0	10.1	3.4×10^{-7}	2.9×10^{-5}
(324 K)	2	27	3.4	10.9	5.0×10^{-5}	1.3×10^{-6}
	3	66	4.4	11.6	4.2×10^{-4}	3.8×10^{-7}
	4	3	6.5	11.2	1.1×10^{-4}	5.9×10^{-8}

[a] ΔG° is the equilibrium free energy difference $\Delta G^\circ_{\mu\nu}$ defined in eq 24 for PCET. [b] λ_o is the outer-sphere reorganization energy $(\lambda_o)_{\mu\nu}$ defined in eq 26 for PCET. [c] V is the coupling $V_{\mu\nu}$ defined in eq 27 for PCET. [d] $\Delta G^\ddagger$ is the sum of the work w_r defined in eq 10 and the free energy barrier defined in eq 23 for PCET.

the proton vibrational states are identical to the energies of the free energy surfaces at these solvent coordinates. Although the lowest proton vibrational wave function is localized in the *b* well, the higher proton vibrational wave functions become more delocalized and thus have greater amplitude in the *a* well. As discussed in ref 49, the relative contributions of these product states to the overall PCET rate are determined by a competition between the couplings, which favor product states with more *a* character, and the equilibrium free energy differences, which favor the lowest energy product state that has more *b* character. The couplings favor product states with more *a* character due to the averaging over the reactant and product proton vibrational wave functions. If the reactant proton vibrational wave function is localized in the *a* well, the overlap between the reactant and product proton vibrational wave functions will increase as the amplitude of the product vibrational wave function near the *a* well increases.

Table 2 presents a detailed analysis of the contribution of each product state to the PCET rate for H transfer at 298 and 324 K and for D transfer at 324 K. The value of w_r, the work to form the reacting complex, is 1.35 kcal/mol at 298 K and 1.50 kcal/mol at 324 K. Note that the outer-sphere reorganization energies range from 10.1 to 11.6 kcal/mol for the various product states. These values differ from the value for pure EPT ($\lambda^{EPT}_{1a\rightarrow 2b} = 5.8$ kcal/mol) given in Table 1 due to mixing of the *a* and *b* PT states in both the reactant and product ET diabatic states. For both H and D transfer, the percentage of 1*a* character in the intersecting region for the lowest reactant state is 68%. For H transfer, the percentages of 2*b* character in the intersecting region for the first, second, and third product states are 68%, 53%, and 54%, respectively. For D transfer, the percentages of 2*b* character in the intersecting region for the first, second, and third product states are 68%, 61%, and 49%, respectively. These trends are illustrated in Figure 5, where a greater percentage of 2*b* character corresponds to a larger amplitude of the vibrational wave function near the *b* well.

The relative contributions of each product state to the PCET rate are determined by a competition between the couplings and the free energy barriers. At 298 K, the first product state (i.e., the ground state) contributes 53% to the rate, while the second product state contributes the majority of the remaining 47%. The lower free energy barrier favors the first product state, while the larger coupling favors the second product state, and these two effects nearly balance for this system. At 324 K, the first product state contributes only 45% to the rate since the impact of the difference in free energy barriers on the relative contributions to the rate is smaller at higher temperatures. For deuterium transfer at 324 K, the first product state contributes only 4% to the rate, and the second and third product states make the largest contributions. As shown in Figure 5, the smaller zero-point energy for deuterium leads to higher localization of the deuterium ground state vibrational wave function. The smaller contribution of the first product state for deuterium transfer is due to the smaller overlap of the reactant and product deuterium vibrational wave functions, leading to a much smaller coupling for the product ground state with deuterium than for that with hydrogen. The second and third product states for deuterium are close enough in energy that they both contribute significantly to the rate. The significant contribution of these delocalized states leads to the moderate deuterium kinetic isotope effect of ~2.3 that has been measured experimentally and calculated with our theory.

Table 3. Comparison of the Single ET and PCET Reactions (Energies in kcal/mol)

	k_{bi} [a] ($M^{-1}\,s^{-1}$)	w_r [b]	λ_i [c]	λ_o [d]	V^2 [e]	$e^{-\Delta G^\ddagger/k_BT}$ [f]
ET	1.7×10^4	2.02	10.8	13.1	6.3×10^{-4}	1.4×10^{-6}
PCET	5.8×10^3	1.35	10.8	10.1	9.6×10^{-6}	1.5×10^{-5}
		1.35	10.8	11.5	3.4×10^{-4}	3.6×10^{-7}

[a] k_{bi} is the experimentally measured bimolecular rate constant of the ET or PCET reaction given in eq 1 or 3, respectively, at 298 K. [b] w_r is the work required to form the precursor complex in solution. [c] λ_i is the inner-sphere reorganization energy for the Fe−N bonds. [d] λ_o is the outer-sphere reorganization energy $\lambda_{1\rightarrow 2}$ for ET and $(\lambda_o)_{\mu\nu}$ defined in eq 26 for PCET. [e] V is the coupling V_{12} for ET and the coupling $V_{\mu\nu}$ defined in eq 27 for PCET. [f] $\Delta G^\ddagger$ is the sum of the work w_r defined in eq 10 and the free energy barrier defined in eqs 17 and 23 for ET and PCET, respectively.

Discussion

The similar rates for single ET and PCET arise mainly from the balance between the difference in outer-sphere reorganization energies and the difference in couplings. Table 3 presents a detailed comparison of the single ET and PCET reactions at 298 K. The contributions from both the first and second product states are given for the PCET reaction. As shown in Table 2, both states contribute significantly to the overall PCET rate.

The most important comparison between single ET and PCET concerns PCET for the dominant first product state. In this case, the total free energy barrier $\Delta G^\ddagger$ is smaller for PCET than for ET since the work term w_r for the formation of the precursor complex is 0.7 kcal/mol smaller for PCET and the outer-sphere reorganization energy is 3.0 kcal/mol smaller for PCET. This lower free energy barrier increases the rate of PCET relative to that of ET. The coupling is smaller for PCET than for ET due to the averaging over the reactant and product proton vibrational wave functions in the coupling for PCET. The overlap of the reactant and product proton vibrational wave functions is particularly small for the first product state since the reactant and product wave functions are localized on opposite sides of the N−N bond (i.e., the reactant is localized in the *a* well and the product is localized in the *b* well). This smaller coupling for PCET decreases the rate of PCET relative to that of ET. For the first product state of the PCET system, the difference in the free energy barriers is nearly compensated by the difference in the couplings, leading to similar rates for single ET and PCET.

A complete analysis of the single ET and PCET reactions requires a comparison between single ET and PCET for the second product state as well. In this case, the total free energy

(49) Decornez, H.; Hammes-Schiffer, S. *J. Phys. Chem. A* **2000**, *104*, 9370.

barrier $\Delta G^{\ddagger}$ is slightly larger for PCET than for ET since the equilibrium free energy difference $\Delta G°$ is 3.5 kcal/mol larger for PCET, while the work term is 0.7 kcal/mol smaller for PCET and the outer-sphere reorganization energy is 1.6 kcal/mol smaller for PCET. The coupling is only slightly smaller for PCET than for ET since the second product state for PCET is delocalized, leading to substantial overlap between the reactant and product proton vibrational wave functions. Hence, for the second product state of the PCET system, the similarity of both the free energy barriers and couplings leads to similar rates for single ET and PCET.

The fundamental differences between the single PT and PCET reactions are that the single PT reaction is electronically adiabatic and requires symmetrization of the proton potential energy curve, while the PCET reaction is electronically nonadiabatic and does not require this symmetrization. Moreover, the outer-sphere reorganization energy is significantly smaller for single PT than for PCET. The basic mechanism for the single PT reaction is that solute reorganization symmetrizes the proton potential energy curve, as shown in Figure 2, to allow the electronically adiabatic proton transfer mechanism. In contrast, as shown in Figure 4b, the PCET reaction does not require this symmetrization of the proton potential energy curve. Although the relative energies of the reactant and product proton vibrational states change, the shapes of the proton potential energy curves do not change significantly along the solvent reaction path for PCET. For all relevant solvent coordinates, the *a* well is lower than the *b* well for the reactant proton potential energy curve, and the reverse is true for the product potential energy curve. This prevailing asymmetry is due to the strong impact of the ET state on the proton potential energy curve (i.e., the electrostatic interaction between the electron donor and acceptor with the proton). Thus, the PCET reaction does not require symmetrization of the proton potential energy curve, as is required for the single PT reaction. Instead, the basic mechanism for the PCET reaction is that solvent reorganization leads to a nonadiabatic transition between two different electronic/proton vibrational states.

The ET, PT, and PCET reactions involve several different types of inner-sphere (solute) reorganization. In our calculations, the inner-sphere reorganization energy due to the Fe−N bonds is assumed to be the same for the ET and PCET reactions. For the PCET reaction, the inner-sphere reorganization due to the motion of the transferring hydrogen atom is included through the quantum mechanical treatment of the hydrogen nucleus. This reorganization influences the coupling given in eq 27 through the reactant and product proton vibrational wave functions. Greater inner-sphere reorganization due to the hydrogen motion leads to smaller overlap between the reactant and product proton vibrational wave functions and thus decreases the coupling and the rate of the PCET reaction. The additional reorganization within the ligands, such as small adjustments of bond lengths and angles upon protonation and deprotonation, is neglected in our PCET calculations. If this additional inner-sphere reorganization energy could be calculated, it could be added to the total reorganization energy, and the coupling parameters could be slightly modified to reproduce the experimental rate for PCET. This contribution is not expected to dominate the PCET reaction, however, due to the strong effect of the ET state on the asymmetry of the proton potential energy curve. In contrast, the inner-sphere reorganization within the ligands plays an important role in the PT reaction due to the required symmetrization of the proton potential energy curve for the electronically adiabatic mechanism.

One of the strengths of the analysis presented in this paper is that it is not strongly dependent on the specific parameters in the model. If different values of the work term w_r, the electronic coupling V^{ET}, and the inner-sphere reorganization energy λ_i were used consistently in the ET and EPT models, the trends would not change. For example, if V^{ET} were known, λ_i could be fit to reproduce the rate of single ET. If these alternative parameters were used to calculate the rate of PCET, the experimental PCET rate would be obtained with only a very minor (if any) adjustment of V^{PT}. In addition, if the prefactor P_r defined in eq 14 were calculated with an alternative expression, the coupling V^{ET} could be adjusted to maintain the same rate of single ET. Thus, this theory reproduces the experimentally determined relationshoip between the PCET and ET rates regardless of specific choices of parameters.

These theoretical calculations also reproduce the experimentally determined deuterium kinetic isotope effect of 2.3 ± 0.3 for the PCET reaction. Higher kinetic isotope effects of up to ~35 have been measured for other PCET reactions, such as those of oxoruthenium complexes.[11−13] The kinetic isotope effect for this iron bi-imidazoline system is moderate due to the short distance (~2.67 Å) between the proton donor and acceptor. A short proton transfer distance leads to a low barrier along the proton coordinate and partially delocalized ground state proton vibrational wave functions, as well as contributions from delocalized excited proton vibrational states. As a result, the reactant and product proton vibrational wave functions overlap significantly, even for the lowest energy product state, for which they are localized on different sides of the proton transfer interface. This theory predicts that the kinetic isotope effect would increase if the proton transfer distance were increased, leading to a higher and wider barrier along the proton coordinate and thus to more separated and localized proton vibrational wave functions. When the proton transfer distance is increased too much, however, the proton transfer reaction will no longer occur, and the mechanism will be ET rather than PCET. Thus, the maximum kinetic isotope effect is expected to occur for intermediate proton transfer distances of ~2.8 Å.

Conclusions

The theoretical calculations presented in this paper allow a comparison of the single ET, single PT, and PCET reactions in iron bi-imidazoline complexes. In this formulation, the ET reactions are electronically nonadiabatic, while the PT reactions are electronically adiabatic. The transferring hydrogen nucleus is treated quantum mechanically. The outer-sphere (solvent) reorganization energies are calculated with the FRCM method and are found to be ~13, ~2, and ~11 kcal/mol for ET, PT and PCET reactions, respectively. The relatively large outer-sphere reorganization energy for PCET indicates a significant change in solute charge distribution during PCET, which suggests that this is not a true "hydrogen atom" transfer. This theory accurately reproduces the relative rates of the three types of reactions, as well as the deuterium kinetic isotope effect for PCET.

Within this theoretical framework, the rate expressions for single ET and PCET reactions are formally similar. In both cases, the rate is proportional to the square of the coupling and inversely proportional to the free energy barrier, which depends on both outer-sphere (solvent) and inner-sphere (solute) reorganization energies. The outer-sphere reorganization energy calculated with the FRCM method is ~1−3 kcal/mol lower for PCET than for ET due to the larger change in charge distribution for ET. The inner-sphere reorganization energy involving the

Fe−N bonds is assumed to be the same (∼11 kcal/mol) for ET and PCET. The coupling between ET states is also assumed to be the same for ET and PCET. In the case of PCET, however, this coupling is averaged over the reactant and product proton vibrational wave functions.

This theoretical formulation indicates that the relative rates of ET and PCET in the iron bi-imidazoline systems are determined predominantly by a balance between two factors. The first factor is the outer-sphere (solvent) reorganization energy, which is larger for ET than for PCET and hence increases the rate of PCET relative to ET. The second factor is the coupling, which is smaller for PCET due to averaging over the reactant and product proton vibrational wave functions and hence decreases the rate of PCET relative to ET. Thus, the similarity of the rates for ET and PCET is due mainly to the compensation of the smaller outer-sphere reorganization energy for PCET by the larger coupling for ET.

The mechanism for the single PT reaction is fundamentally different from the mechanism for the PCET reaction. The single PT reaction is found to have no free energy barrier along the collective solvent coordinate due to the very small outer-sphere reorganization energy. Thus, solute reorganization dominates the single PT reaction. In particular, the bond lengths and angles within the ligands must reorganize to symmetrize the proton potential energy profile. (Note that for the single PT system, the oxidation state of the iron atoms is the same on both sides of the proton transfer interface.) The single PT reaction is found to be electronically and vibrationally adiabatic. In contrast, the PCET reaction is electronically nonadiabatic and does not require symmetrization of the proton potential energy profile by solute reorganization. The proton potential energy profile is highly asymmetric along the PCET reaction path due to the asymmetry of the ET states (i.e., the oxidation state of the iron atoms is different for the two sides of the proton transfer interface). In the PCET mechanism, the solvent reorganization alters the relative energies of the proton vibrational states and allows the proton to tunnel during nonadiabatic transitions between the ET states. Excited vibrational product states have also been found to participate in the PCET reaction. These mechanistic differences account for the faster rate of single PT compared to PCET.

The results in this paper illustrate the importance of feedback between experiment and theory. The agreement between experiment and theory for these iron bi-imidazoline complexes provides validation for the theory. In turn, the theory offers predictions that are experimentally testable. For example, the theory predicts that the kinetic isotope effect and the rate of ET relative to PCET will increase as the proton transfer distance increases (until the distance is so large that it prohibits the proton transfer reaction) and as the electron transfer distance decreases. Both of these alterations increase the height and width of the barrier along the proton coordinate, leading to more separated and localized proton vibrational wave functions and smaller couplings for PCET. The testing of these predictions and the subsequent refinement of the theory will continue to enhance our understanding of PCET reactions.

Acknowledgment. We thank Dr. Alexander Soudackov, Dr. Ivan Rostov, Dr. Simon Webb, and Dr. Mark Kobrak for stimulating discussions. We also thank Dr. Justine Roth and Dr. Jim Mayer for helpful comments about this manuscript. We are grateful for financial support from NSF Grant CHE-0096357. S.H.-S. is the recipient of an Alfred P. Sloan Foundation Research Fellowship and a Camille Dreyfus Teacher-Scholar Award.

JA0100524